**Seventh International Conference on Computational Fluid Dynamics (ICCFD7), Big Island, Hawaii, July 9-13, 2012**

**ICCFD7-3705**

# Dynamic Model of Vortex Cavitation based on Axisymmetric Navier-Stokes Equation

K. Ito*, T. Ezure*, S. Ohno* and H. Kamide*
Corresponding author: ito.kei@jaea.go.jp

* Japan Atomic Energy Agency, Japan

**Abstract:** In this paper, a new dynamic model of vortex cavitation is proposed as an approximate solution of the unsteady axisymmetric Navier-Stokes equation. This model provides unsteady behaviors of a sub-surface vortex, i.e., development of the vortex, occurrence of the vortex cavitation, evolution and contraction of the cavitating radius. In addition, the effect of surface tension is considered in the model. The simulation results under steady and fluctuating far-field pressure conditions show that the model has the ability to simulate the vortex cavitation.

*Keywords:* Vortex Cavitation, Axisymmetric Navier-Stokes Equation, Cavitation Model, Surface Tension, Cavitating Radius.

## 1 Introduction

The cavitation due to a sub-surface vortex can be observed in a lot of industrial scenes, such as a pump intake or a tip of impeller blade. A great deal of studies has been conducted to suppress the cavitation occurrence because noise, vibration and/or erosion can be induced by such vortex cavitaion. Also in our study on sodium-cooled fast reactors, the vortex cavitaion near the intake mouth of the outlet pipe from the reactor vessel is investigated experimentally and numerically to establish the cavitation-free design [1,2]. However, the direct numerical simulation of the vortex cavitation has a great difficulty, that is, the cavitating radius is often very small to require an unrealistically fine mesh for an accurate numerical simulation. In such a case, it is preferable to simulate the vortex cavitation with a cavitation model. In general, the cavitation is modeled by the Rayleigh-Plesset (R-P) equation [3,4] which gives the dynamic bubble behavior with the assumption of spherical symmetry [5-7]. This R-P model can be applied to the vortex cavitation [8,9], but in such cases, the vortex cavitaiton is simulated as a series of spherical bubbles in a line along the vortex core. Such a simulation may give an important insight into the vortex cavitation behavior. However, for an accurate numerical simulation of the vortex cavitation, physically more realistic model should be employed.

In this paper, the authors propose a new dynamic modeling of the vortex cavitation based on the axisymmetric unsteady Navier-Stokes (N-S) equation. In concrete term, an approximate solution of the N-S equation is derived and used to calculate the radial pressure distribution. Then, the cavitating radius is determined by comparison of the calculated pressure distribution with vapor pressure in consideration of time-delay in phase change. The surface tension is also considered in the model to calculate the cavitating radius accurately. Several simulations are performed under various far-filed and surface tension conditions to confirm the physical adequacy of the proposed cavitation model.

# 2 Dynamic Vortex Cavitaion Model

## 2.1 Modeling of Sub-surface Vortex

In the dynamic cavitation model, the velocity distribution of a sub-surface vortex is modeled by the unsteady axisymmetirc N-S equation. Namely, the velocity field is assumed to be axisymmetric along the vortex core. In addition, the uniform axial velocity in radial direction is assumed as well as the famous Burgers vortex model [10]. With these assumptions, the equation of the circumferential velocity ($v$) is written as

$$\frac{\partial v}{\partial t}-\frac{1}{2}\alpha\frac{\partial}{\partial r}(rv)+\frac{C}{r^2}\frac{\partial}{\partial r}(rv)=\upsilon\frac{\partial}{\partial r}\left\{\frac{1}{r}\frac{\partial}{\partial r}(rv)\right\}$$

where $\alpha$ is the axial velocity gradient, $\upsilon$ is the kinetic viscosity. As shown below, $C$ is the function of the cavitating radius $R$ and its time derivative $\dot{R}$ (= $dR/dt$), which represent the effect of the cavitation on the velocity distribution.

$$C=\frac{1}{2}\alpha R^2+R\dot{R}$$

This equation is derived from the continuity equation in consideration of the velocity condition at a gas-liquid interface. The equation of the circumferential velocity is re-written in the form of the axial vorticity ($\omega$) as

$$\frac{\partial\omega}{\partial t}-\frac{1}{2}\alpha r\frac{\partial\omega}{\partial r}-\alpha\omega=\upsilon\frac{1}{r^{C'+1}}\frac{\partial}{\partial r}\left(r^{C'+1}\frac{\partial\omega}{\partial r}\right)$$

where $C' = C/\upsilon$. When $C'$ is temporally constant, this equation can be solved rigorously [11,12]. However, this is not the case with the vortex cavitation as shown above. Therefore, in this paper, the authors employ an approximate solution of the axial vorticity equation with the assumption of small cavitating radius and velocity. Such assumptions are considered to be valid for the vortex cavitation which has very thin cavitating region along the vortex core and relatively slow cavitating velocity ($\dot{R}$) dominated by the sub-surface vortex development. Therefore, the approximate solution can be written as

$$\omega=\frac{1}{1+T'\exp(-\alpha t)}\frac{\Gamma_\infty}{\pi r_0}\exp\left(-\frac{1}{1+T'\exp(-\alpha t)}\frac{r^2-R^2}{r_0^2}\right)$$

and in the form of the circumferential velocity,

$$v=\frac{1}{1+T'\exp(-\alpha t)}\frac{\Gamma_\infty}{2\pi r}\left\{1-\exp\left(-\frac{1}{1+T'\exp(-\alpha t)}\frac{r^2-R^2}{r_0^2}\right)\right\}$$

where $\Gamma_\infty$ is the far-field circulation, $T'$ is the constant determined by an initial condition and $r_0$ ($=2\sqrt{\upsilon/\alpha}$) is the specific radius of the vortex. It is not difficult to check that above solutions establish the differential equations of the circumferential velocity and the axial vorticity when $(R/r_0)^2 << 1$ and $\dot{R} << 1$. In these equations, the superficial specific radius is defined as

$$r_s=r_0\sqrt{1+T'\exp(-\alpha t)}$$

The development and/or attenuation of the sub-surface vortex are calculated by these equations in the dynamic vortex cavitation model.

## 2.2 Modeling of Cavitation

The approximate equation of the circumferential velocity gives the circumferential velocity distribution for each instant of time based on the given cavitating radius at the instant. However, the development of the cavitating radius can not be determined by the approximate equation, and therefore, the cavitating radius for each instant of time has to be determined independently. In this paper, the cavitating radius is calculated by the comparison of radial pressure distribution and vapor pressure. First, the radial pressure distribution is calculated by substituting the approximate equation of the circumferential velocity into the balance equation between centrifugal force and pressure

gradient, which is written as

$$\frac{v^2}{r} = \frac{1}{\rho}\frac{\partial p}{\partial r}$$

where $\rho$ is the liquid density. The resulting pressure distribution is

$$p(r) = p_\infty - \rho\int_r^\infty \frac{v^2}{r}dr$$

where $p_\infty$ is the far-field pressure. Then, the cavitating radius can be determined as

$$p(R) = p_v$$

where $p_v$ is the vapor pressure. However, this equation makes calculation results unstable, i.e. the temporal fluctuation of the cavitating radius is induced because this equation gives very fast cavitating velocity which is not appropriate for the vortex cavitation (as described in Section 2.1). Therefore, the time-delay in phase change should be considered in the dynamic vortex cavitation model. In this study, the time-delay is introduced as a first-order lag equation in consideration of the time constant of the sub-surface vortex development. Namely, since the time evolution of the approximate vortex solution is dominated by the term $\exp(-\alpha t)$, the first-order lag equation is formulated as

$$R(t+\delta t) = R(t) + \{R'(t+\delta t) - R(t)\}\{1-\exp(-\alpha\delta t)\}$$

where $\delta t$ is the time increment in a calculation. This equation calculates the cavitating radius at $t+\delta t$ reduced by considering the time-delay, i.e. $R(t+\delta t)$, from the radius given by the equation $p(R) = p_v$, i.e. $R'(t+\delta t)$, and the radius at $t$, i.e. $R(t)$.

When the effect of the surface tension is not negligible, the comparison of the radial pressure distribution and vapor pressure is conducted by the equation with the surface tension which is written as

$$p(R) = p_v - \frac{\sigma}{R}$$

where $\sigma$ is the surface tension coefficient.

The dynamic behavior of the vortex cavitation is calculated by the combination of two models, i.e. the sub-surface vortex model (Section 2.1) and the cavitation model (this section).

# 3 Verification

## 3.1 Development of Vortex Cavitation

As a basic test of the dynamic vortex cavitation model, the development of the vortex cavitation is calculated. In this calculation, $\Gamma_\infty$ is $0.10\pi$, $\alpha$ is 1.0, $\upsilon$ is $1.0 \times 10^{-6}$, $\rho$ is 1,000, $\sigma$ is 0.0 (without the surface tension), $p_\infty$ is $4.0 \times 10^5$, $p_v$ is $3.0 \times 10^4$.

Figure 1 shows the development of the circumferential velocity. Initially, the circumferential velocity is almost zero, and then, the velocity grows with time to converge on the velocity distiribution almost the same as that of the the Burgers vortex model [10] around $t$ = 15.0. The discrepancy between the Burgers vortex and the calculated circumferential velocity distirubtion at $t$ = 15 is observed near the vortex center because the cavitating region exists in the calculation result. Figure 2 shows the development of the cavitating radius. Before $t$ = 10.8, no cavitation occurs because the minimum pressure, i.e. the pressure at the vortex center, is larger than the vapor pressure. After the minimum pressrue reaches the vapor pressure, the cavitating radius grows dependent on the cicumferential velocity development. Finally, the cavitating radius converges on the constant value of $4.52 \times 10^{-4}$ at around $t$ = 15.0 because the circumferential velocity does not grow any more. This result shows that the dynamic vortex cavitation model can calculate the cavitation occurrence accompanied by the sub-surface vortex development.

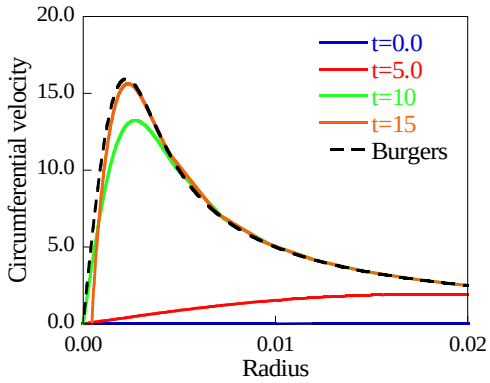


Figure 1: Development of circumferential velocity.

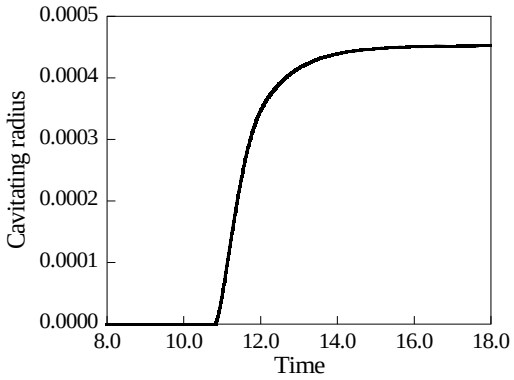


Figure 2: Development of cavitating radius.

## 3.2 Effect of Surface Tension

The surface tension works to suppress the vortex cavitation because the pressure reduction necessary to induce the vortex cavitation is enhanced by the surface tension. In this section, the similar calculation to that in the previous section but $\sigma$ is 5.0 is performed to see the effect of the surface tension.

Figure 3 shows the comparison of the cavitating radius development with and without the surface tension. As expected, the vortex cavitation is suppressed by the surface tension. Namely, the onset of the cavitation is delayed from $t$ = 10.8 (without the surface tension) to $t$ = 11.2 (with the surface tension), and the convergent value is reduced from $4.52 \times 10^{-4}$ (without the surface tension) to $4.04 \times 10^{-4}$ (with the surface tension). This reduction of the cavitating radius can change the circumferential velocity distribution. However, such effect is negligible as shown in Figure 4 (the comparison of the circumferential velocity development with and without the surface tension). It is natural that the circumferential velocity distributions coincide at $t$ = 10.0 because there is no cavitation at this time, but the velocity distributions are almost the same also at $t$ = 15.0.

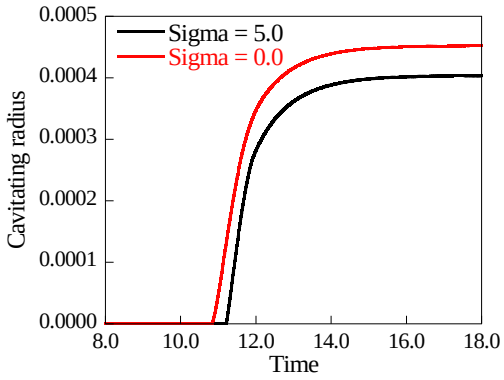


Figure 3: Comparison of cavitating radius development (effect of surface tension).

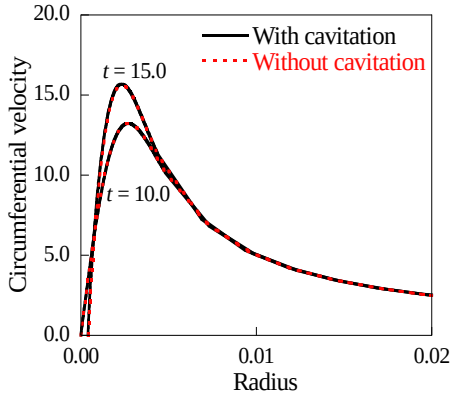


Figure 4: Comparison of circumferential velocity (effect of surface tension).

### 3.3 Calculation with Fluctuating Far-field Pressure

When the far-field pressure fluctuates temporally, the cavitation radius is expected to fluctuate as well. In this section, the far-field pressure is defined by the sinusoidal function as

$$p_\infty(t) = p_\infty(0) + A\sin\{2\pi k(t - t_s)\}$$

and the temporal fluctuation of the cavitating radius is investigated. It should be mentioned that the far-field pressure fluctuation starts at $t$ = 12.0 when the strength of the sub-surface vortex is considered to be sufficiently high.

Figure 5 shows the calculation result of the cavitating radius which fluctuates in synchronization with the far-field pressure. In fact, the frequency of the cavitating radius fluctuation is the same as that of the far-field pressure, so that the trend is clear that the lower the far-field pressure, the larger the cavitating radius. This result is valid because the dynamic vortex cavitation model is constructed based on the incompressible N-S equation, and therefore the compressibility of the gaseous region is not considered in the model.

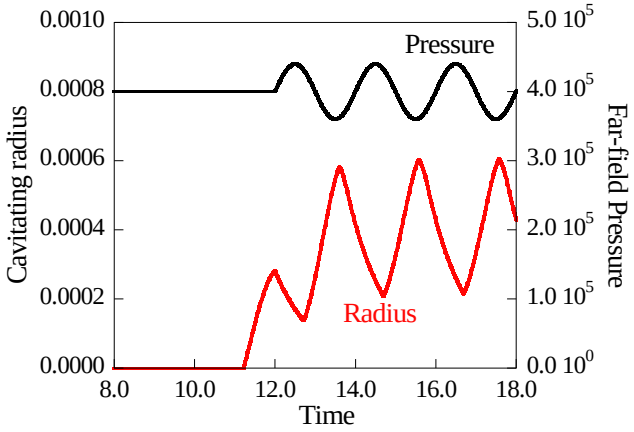


Figure 5: Time fluctuation of cavitating radius and far-field pressure.

## 3 Conclusion and Future Work

The several simulation results show that the proposed dynamic cavitation model provides physically appropriate behaviors of the vortex cavitation. This fact implies that the model is developed in a proper manner from the N-S equation. As a future work, the model will be incorporated into our three-dimensional CFD code [13,14] which simulates gas-liquid two-phase flows by a high-precision volume-of-fluid algorithm. Then, the numerical simulations of sub-surface vortices are performed to validate the reproducibility of the vortex cavitation by the CFD code.

## References

[1] T. Ezure, N. Kimura, J. Kobayashi and H. Kamide, Experimental study on influences of kinematic viscosity on occurrences of cavitation due to sub-surface vortex", Proceedings of the 14th International Topical Meeting on Nuclear Reactor Thermalhydraulics, Toronto, Canada, September 25-30, 2011.

[2] T. Ezure, K. Ito, T. Onojima, N. Kimura and H. Kamide, Fundamental behavior of vortex in small-scaled SFR upper plenum model -Influences of kinematic viscosity and system pressurization on vortex cavitation-, Proceedings of the Seventh Korea-Japan Symposium on Nuclear Thermal Hydraulics and Safety, Beppu, Japan, December 9-12, 2012 (to be published).

[3] M. S. Plesset and A. Prosperetti, Bubble dynamics and cavitation, Annual Review of Fluid Mechanics, 9:145-185, 1977.

[4] A. Prosperetti and M. S. Plesset, Vapour-bubble growth in a superheated liquid, Journal of Fluid Mechanics, 85:349-368, 1978.

[5] A. K. Singhal, M. M. Athavale, H. Li and Y. Jiang, Mathematical basis and validation of the full cavitation model, Journal of Fluids Engineering, 124:617-624, 2002.

[6] A. Hosangadi and J. Ahuja, A new unsteady model for dense cloud cavitation in cryogenic fluids, Proceedings of 17th AIAA Computational Fluid Dynamics Conference, Toronto, Canada, June 6-9, 2005.

[7] N. Tsurumi, Y. Tamura and Y. Matsumoto, Bubble model for cavitating flow simulation including high void fraction region, Proceedings of fifth European Conference on Computational Fluid Dynamics, Lisbon, Portugal, June 14-17, 2010.

[8] C. T. Hsiao and G. L. Chahine, Numerical study of cavitation inception due to vortex/vortex interaction in a ducted propulsor, Proceedings of 25th Symposium on Naval hydrodynamics, St. John's Newfoundland and Labrador, Canada, August 8-13, 2004.

[9] M. A. Maksoud, D. Hanel and U. Lantermann, Modeling and computation of cavitation in vortical flow", International Journal of Heat and Fluid Flow, 31:1063-1074, 2010.

[10] J. M. Burgers, A mathematical model illustrating the theory of turbulence, *Advance in applied*

*mechanics* (edited by R. Mises and T. Karman), Academic Press ING., New York, 1948.

[11] T. Kambe, Axisymmetric vortex solution of Navier-Stokes equation, Journal of the Physical Society of Japan, 53:13-15, 1984.

[12] Y. Fukumoto, General unsteady circulatory flow outside a porous circular cylinder with suction or injection, Journal of the Physical Society of Japan, 59:918-926, 1990.

[13] K. Ito, T. Kunugi, H. Ohshima and T. Kawamura, Formulations and validations of a high-precision volume-of-fluid algorithm on non-orthogonal meshes for numerical simulations of gas entrainment phenomena, Journal of Nuclear Science and Technology, 46:366-373, 2009

[14] K. Ito, T. Kunugi and H. Ohshima, High-precision reconstruction of gas-liquid interface in PLIC-VOF framework on unstructured mesh, *Computational Fluid Dynamics 2010* (edited by A. Kuzmin), 563-567, 2011.